Simulation of straight and bent self-written waveguides in photopolymer mixture using phenomenological and diffusion models

Monali Suar, Maik Rahlves, Eduard Reithmeier, Bernhard Roth

Monali Suar, Maik Rahlves, Eduard Reithmeier, Bernhard Roth , "Simulation of straight and bent self-written waveguides in photopolymer mixture using phenomenological and diffusion models," Proc. SPIE 10690, Optical Design and Engineering VII, 106900D (5 June 2018); doi: 10.1117/12.2312507

SPIE.

Event: SPIE Optical Systems Design, 2018, Frankfurt, Germany

Simulation of Straight and Bent Self-Written Waveguides in Photopolymer Mixture Using Phenomenological and Diffusion Models

Monali Suar[a], Maik Rahlves[a], Eduard Reithmeier[b], and Bernhard Roth[a]

[a]Hannover Centre for Optical Technologies, Leibniz Universität Hannover, Nienburger Str. 17, 30167 Hanover, Germany

[b]Institute of Measurement and Automatic Control, Leibniz University Hanover, Nienburger Str. 17, 30167 Hanover, Germany

ABSTRACT

Straight and bent self-written waveguides (SWWs) are formed within a photomonomer mixture by means of a self-trapping effect when a single laser beam or two laser beams with tilt are propagated inside. These SWWs can be used as optical interconnects in integrated photonic circuits if two laser beams are launched in opposite directions into the photomonomer. In this work, two kinds of photo-polymerization models are implemented to simulate the SWWs. In the phenomenological model, the refractive index increases directly with actinic laser intensity, whereas the diffusion model has a more complex variation of refractive index profile which takes into account the individual redistribution of mixture components. Both these models are linked with a Crank-Nicholson based Beam Propagation Method (CN-BPM) to simulate the time varying light distribution within the polymer coupling structures. Differences are observed in the numerical simulation results for straight and bent SWWs with respect to the temporal evolution of refractive index within the mixture, corresponding beam intensity profiles and curing time. In addition, we show that a saturation of refractive index change leads to the polymerization of surrounding monomer and, as consequence, to corrupted light guiding. We report on the minimum refractive index modulation that is required for optimal light guiding within the SWW.

Keywords: Self-trapping, Self-action effects of light, Polymer waveguides

1. INTRODUCTION

The physics of self-writing of waveguides is a combined outcome of self-focusing and self-trapping effects of light. Many experimental and theoretical studies have already been performed to understand the underlying self-writing phenomenon of light in photomonomer as well as in photosensitive material media.[1–4] An induced change in refractive index occurs within the material as the light propagates through it. Initially, the laser beams diffract freely which is compensated at the later stage by the induced increase in refractive index due to polymerization of the monomer along the propagation axis. This induced change in refractive index is maximum where the beam intensity is maximum. The maxima of the refractive index are located near the exit ports of the Gaussian beams. The induced change in refractive index later becomes sufficient to self-focus and self-trap the beam along the propagation axis to create a waveguide-like optical channel. Once the optical channel is established, it remains within the medium and it is possible to propagate any optical beam of different wavelengths. Such light-induced waveguides are often referred to as self-written waveguides (SWWs).

A single optical channel results within the material mixture by illumination with one Gaussian laser beam and it is referred to as straight SWW.[5,6] When two Gaussian beams with offset or misalignment along the transverse x-direction are propagated into the material mixture from opposite directions, the two optical channels are self-bent to compensate the misalignment and merge to create a single channel. Such resulting channels are referred as bent SWWs.[4,7]

Further author information: (Send correspondence to Email: monali.suar@hot.uni-hannover.de, Telephone: +49 511 762-14686)

Optical Design and Engineering VII, edited by Laurent Mazuray, Rolf Wartmann, Andrew P. Wood, Proc. of SPIE Vol. 10690, 106900D · © 2018 SPIE
CCC code: 0277-786X/18/$18 · doi: 10.1117/12.2312507

Two theoretical material models are implemented in this work to simulate such straight and bent SWWs. These two material models are then linked with the Crank-Nicholson based Beam Propagation Method (CN-BPM) to obtain the light distributions within the SWWs. The numerical simulations allow us to predict the temporal dynamics of the induced change in refractive index and corresponding beam intensity distributions for SWWs. We present a comparative study for refractive index modulation, intensity distributions and curing times for the SWWs using Model 1 and Model 2.

2. NUMERICAL MODEL

2.1 Optical Simulation

To calculate the light distribution of self-growing optical channels, a two- dimensional scalar beam propagation method (2D-BPM) is implemented, inspired by the work of Pedrola.[8] This method is nonlocal in time which is obtained by assuming a slowly varying field envelope and applying the paraxial approximation to the Helmholtz equation:

$$2in_0k_0\frac{\partial u(x,z)}{\partial z} = \frac{\partial^2 u(x,z)}{\partial^2 x} + k_0^2(n^2 - n_0^2)u(x,z). \tag{1}$$

A Crank-Nicholson based finite difference scheme with transparent boundary condition is applied to Eq. (1) to obtain the numerical solution. Here, n_0 is the initial average value of the refractive index of the homogeneous medium and n is the current refractive index of the material mixture which is a dynamic value and obtained by solving the material model equations presented later in this section. k_0 is the free space wavenumber and calculated from the beam wavelength λ via $k_0 = 2 * \pi/\lambda$. $u(x,z)$ is the electric field envelope amplitude, x and z are the transverse and propagation direction, respectively. The above 2D-BPM is coupled with the material models 1 and 2 below. The temporal dynamics of the refractive index of the core of the SWW is obtained by solving the material model equations and then this new value is passed down to the CN-BPM to compute the new field distribution for each time iteration.

2.2 Material Model 1

A simple phenomenological material model is implemented which describes the evolution of the refractive index for the material mixture towards a maximum saturation value for the refractive index modulation. The change in refractive index continues to grow and finally saturates to a maximum modulation value. This process is described by a simple first order differential equation, Eq.(2), where the induced modification in refractive index increases directly with the actinic intensity of the writing beams:

$$\frac{\partial \Delta n(x,z,t)}{\partial t} = A_s I(x,z,t)^p \left(1 - \frac{\Delta n(x,z,t)}{\Delta n_s}\right). \tag{2}$$

Here, t is the elapsed exposure time, Δn_s is the fixed saturation value of refractive index modulation and $I(x,z,t) = |u(x,z,t)|^2$ is the local light intensity. p is the number of photons involved in the process which is typically assumed to be a linear optical process and hence $p = 1$.[9] The real coefficient A_s depends upon the material properties, the number of photons p and the wavelength of light.

2.3 Material Model 2

The material model 2 has a more complex variation of refractive index which is obtained by taking into account the redistributions of individual components of the material mixture and solves two partial differential equations. In this model, the concentration of monomer is influenced by the diffusion of monomers from dark regions to neighboring bright regions which are simultaneously converted into polymer chains. The evolution of the monomer concentration is described by

$$\frac{\partial M(x,z,t)}{\partial t} = \nabla(D\nabla M(x,z,t) - K_r M(x,z,t) I(x,z,t)\Big(1 - \frac{\triangle n(x,z,t)}{\triangle n_f}\Big). \tag{3}$$

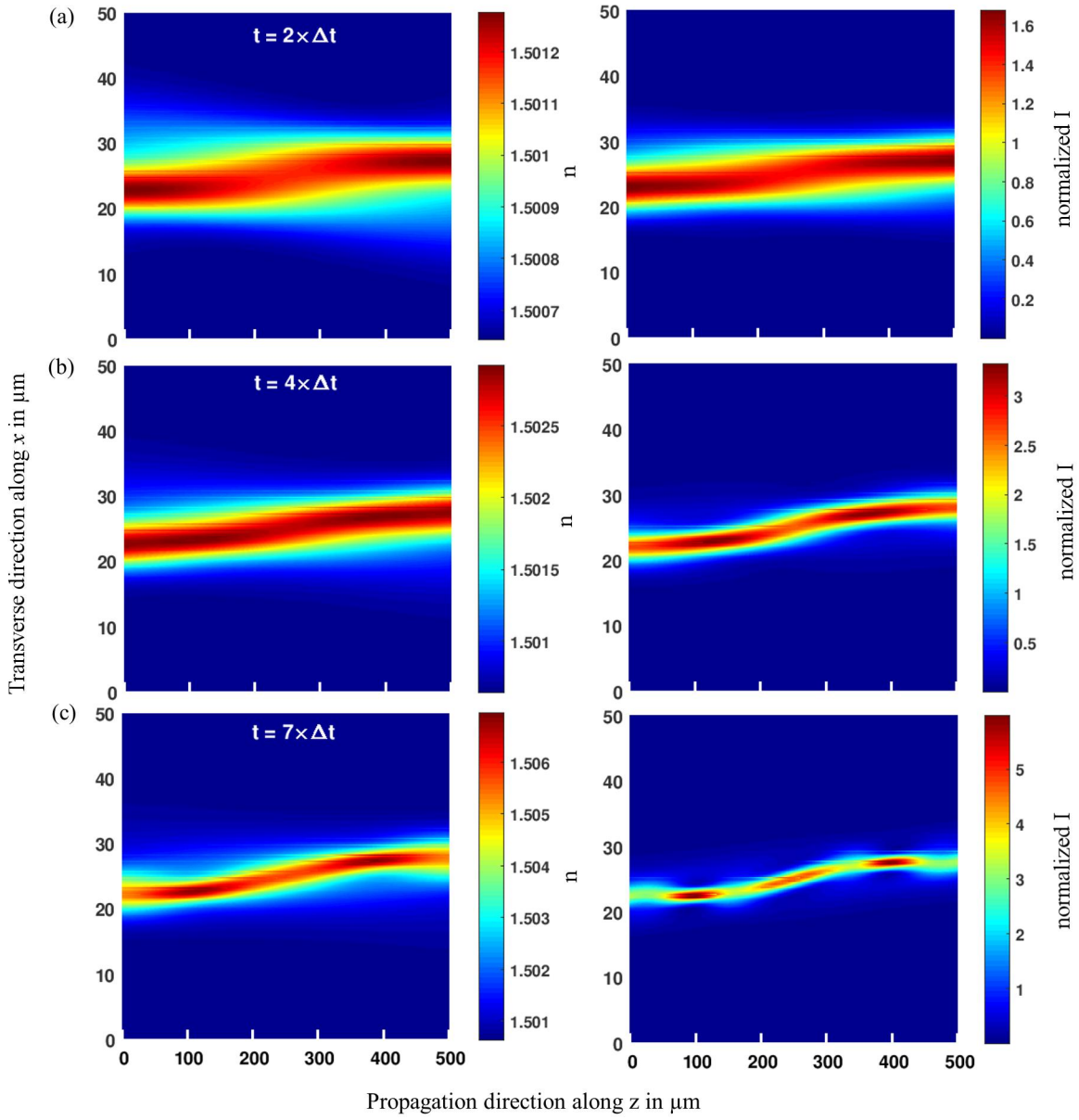

Figure 1. Simulated bent SWW using the diffusion based material model. The refractive index modulation of the evolving core of the SWW is on the left side, the corresponding intensity distributions are on the right side. The intensity was normalized to the maximum intensity of the Gaussian input beam.

As the polymer chains are too heavy to move around, the diffusion coefficient is neglected for polymer evolution and its redistribution within the mixture is governed by

$$\frac{\partial P(x,z,t)}{\partial t} = K_r M(x,z,t) I(x,z,t) \Big(1 - \frac{\triangle n(x,z,t)}{\triangle n_f}\Big). \tag{4}$$

In Eqs.(3) and (4), the monomer and the polymer concentrations are denoted by M, and P, respectively. D is the diffusion constant and K_r is the polymerization rate. The first part in Eq.(3) describes the diffusion of monomer with diffusion constant D and its second part describes the polymerization of monomers to polymer

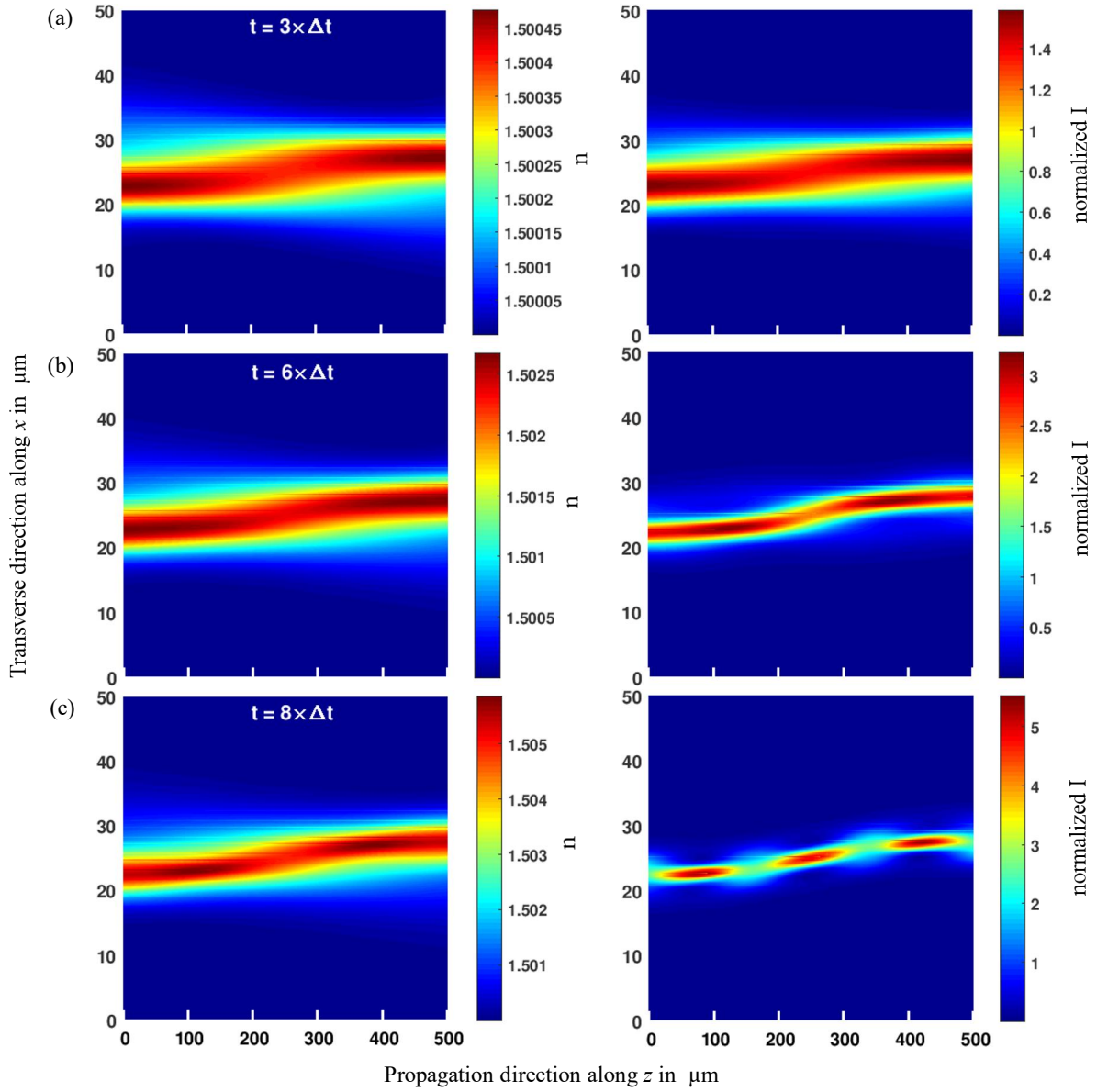

Figure 2. Simulated bent SWW using the phenomenological material model. The refractive index modulation of the evolving core of the SWW is on the left side, the corresponding intensity distributions are on the right side. The intensity was normalized to the maximum intensity of the Gaussian input beam.

chains. $\left(1-\frac{\triangle n(x,z,t)}{\triangle n_f}\right)$ expresses the saturation of the modulation of refractive index and I is the light intensity. Here, the 2D Laplace operator is equal to $\nabla^2 = \frac{\partial^2}{\partial x^2} + \frac{\partial^2}{\partial z^2}$. $\triangle n(x,z,t)$ is the refractive index difference between the core and cladding of the simulated SWW which is a dynamic value and increases till the maximum possible modulation, i.e., $\triangle n_f$ is reached. The maximum modulation $\triangle n_f$ during the simulation is equal to the difference in refractive index n_{max} and n_{min}. Here, n_{max} is the maximum value of the refractive index of the mixture when all monomers are converted into polymer chains and n_{min} is the refractive index of the mixture at the beginning of the simulation prior to the conversion of monomer to polymer chains. By knowing the concentrations of monomer, polymer, and photoinitiator, their refractive index values, densities, and also the corresponding volume fractions are calculated for the individual mixture components. Then, the evolution of refractive index of the material mixture is calculated via the Lorentz-Lorentz relation:[10]

$$\frac{n^2-1}{n^2+2} = \Phi_m \frac{n_m^2-1}{n_m^2+2} + \Phi_p \frac{n_p^2-1}{n_p^2+2} + \Phi_a \frac{n_a^2-1}{n_a^2+2}, \tag{5}$$

where, n_m, n_p and n_a, are the refractive indices of monomer, polymer, and photoinitiator, respectively. Φ_m, Φ_p, and Φ_a, are their corresponding volume fractions. Φ_a is calculated from the conservation principle of total volume fraction, i.e., $\Phi_a = 1 - \Phi_m - \Phi_p$. For details of the calculation process we refer to the work of Babeva et al.[11]

2.4 Numerical Parameters

For models 1 and 2, the simulation starts from a homogeneous refractive index background. In model 1, the change in refractive index continues to grow till Δn equals the maximum modulation value Δn_s. In model 2, the change in refractive index grows in a temporal loop till all monomers are converted into polymer chains. For comparison of the two models, the numerical parameters during the simulation are kept equal. The initial refractive index and maximum change in refractive index possible are also kept constant. In model 1, the simulation starts from a uniform refractive index background with $n_0 = 1.5$ and the maximum modulation is fixed at $\Delta n_s = 0.017$. The coefficient A is set to 1.2×10^{-3}.[6] In model 2, the simulation starts with photomonomer mixture of 40% monomer, 57% polymer, and 3% photoinitiator. The percentages for components are fixed to make sure that the maximum change in refractive index of the mixture is the same as in model 1 after complete conversion of the monomers to polymer chains. The diffusion constant $D = 6 \times 10^{-15}$ m^2/s considered for the simulation was measured experimentally.[12] The polymerization rate K_r is set to 0.6 cm$^2/\mu$W. The refractive index of monomer n_m, polymer n_p, and photo-initiator n_a are fixed at 1.48, 1.52 and 1.46, respectively.[13]

The waist of the Gaussian beams is assumed to illuminate the photopolymer mixture in both models. Two writing Gaussian beams u_1 and u_2 from input facets, $z = 0$ and $z = z_{max}$ are propagated into the mixture to create a bent SWW. However, only one Gaussian laser beam, u_1, is propagated into the mixture in order to create a straight SWW. The initial Gaussian distributions are described as

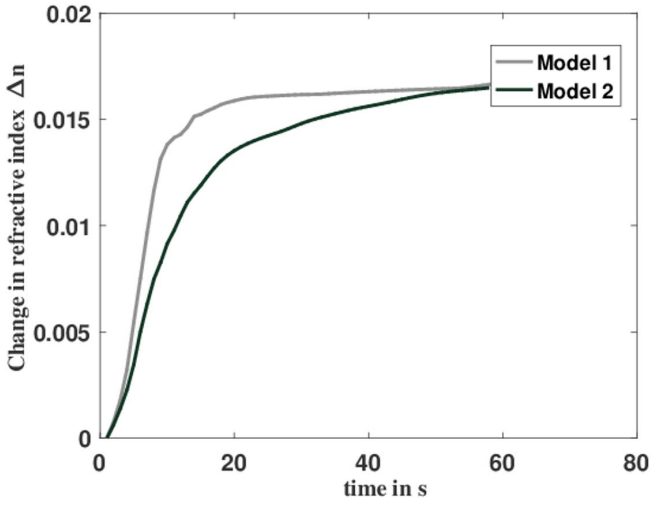

Figure 3. The change in refractive index with curing time for a bent SWW obtained using models 1 and 2, respectively.

$$u_1(x, z = 0, t) = u_0 \exp\left(-\frac{x^2}{a^2}\right), \tag{6}$$

$$u_2(x, z = z_{max}, t) = u_0 \exp\left(-\frac{(x-d)^2}{a^2}\right). \tag{7}$$

Here a is the width of the input Gaussian beams and d is the offset or misalignment length along the transverse direction x, for the case of a bent SWW. The beam width a=5 µm is used for all Gaussian excitations. An offset length of d=5 µm is considered during simulation for both models. The step increments along the transverse direction Δx, the propagation direction Δz, and the time Δt are fixed as 0.5 µm, 1 µm and 0.5s, respectively for both models, which also satisfies the convergence criteria for the finite difference schemes.

3. RESULTS AND DISCUSSION

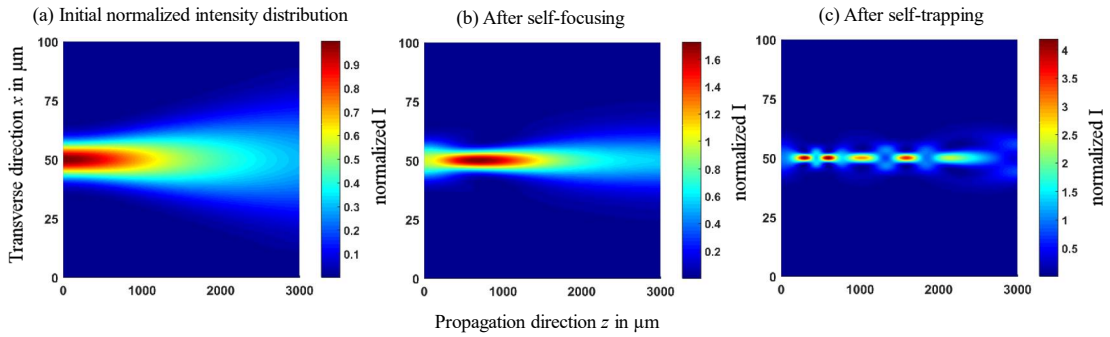

Figure 4. Numerical simulation of a straight SWW within the given material mixture using the phenomenological model. (a) initial normalized light intensity distribution, (b) light intensity distribution after self-focusing of the Gaussian beam, and (c) light intensity distribution when the Gaussian beam is self-trapped.

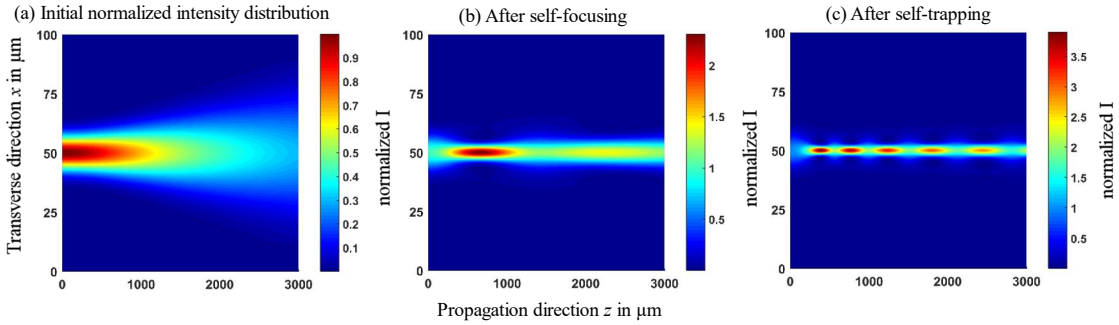

Figure 5. Numerical simulation of a straight SWW within the given material mixture using the diffusion based material model. (a) initial normalized light intensity distribution, (b) light intensity distribution after self-focusing of the Gaussian beam, and (c) light intensity distribution when the Gaussian beam is self-trapped.

3.1 Evolution of bent SWWs

A bent SWW is simulated with both models, as shown in Figs. 1 and 2, respectively. The induced modulation of refractive index of the SWWs and the corresponding beam intensity distribution profiles during the curing process are provided. The simulation started from a uniform refractive index background, i.e. $n = 1.5$, in both models. The diffraction of the propagating beams is strongly compensated when the refractive index along their propagation axis slightly increases from the initial value of 1.5 and the connection is established in the overlapping region of the counter propagating beams, as in Figs. 1(a) and 2(a). When the refractive index along the propagation axis of the beams is further increased to 1.502, the width of bent SWWs decreases further due to the self-focusing effect of the propagating light beam for both models, as shown in Figs. 1(b) and 2(b). The connection established for the diffusion based model has a more uniform surface, see Fig. 1(c), whereas in the phenomenological model, some non-uniformity along the cross-section of the bent SWW can be seen, see Fig. 2(c). Here, the maximum focus points in intensity distribution are referred to as "primary eyes". We also observed that the primary eyes start to move along the propagation axis of the SWWs when the refractive index

of the core of the SWWs increases to 1.505 of beyond starting from the initial refractive index value of 1.5, see Figs. 1(c) and 2(c). This is an indication of good light guiding capabilities of the SWWs and the trajectories of the primary eyes are closely related to the SWW structures.[14] Also, the bending in the curvature of the bent SWW is more prominent in the diffusion based material model, see Fig. 1(c), than in the phenomenological model, see Fig. 2(c).

The change in refractive index $\triangle n$ with curing time for both models, is shown in Fig. 3. $\triangle n$ increases with time for both cases until the maximum saturation of refractive index is reached. The evolution of change in refractive index from $\triangle n = 0$ to $\triangle n = 0.005$ is nearly the same for both models, afterward the evolution in $\triangle n$ is more sharp or steep for model 2 than for model 1, see Fig. 3. There is a slight abrupt near $\triangle n_{max}$ for model 1, whereas, the growth of $\triangle n$ is smoother for model 2.

3.2 Evolution of straight SWWs

A straight SWW is simulated using the two models as well. It is created when a Gaussian beam of width $a = 5\,\mu m$ is traversed through the photopolymer mixture. The maximum intensity of the initial input Gaussian beam is normalized to 1. The results for the straight SWWs are provided in Figs. (4) and (5) for the model 1 and 2, respectively. The initial input Gaussian beam has a significant diffraction within the photopolymer mixture before the simulation started, as shown in Figs. 4(a) and 5(a). As the modulation in the refractive index of the simulated waveguide core increases to the value $n_{core} = 1.502$, from an initial value $n_{core} = 1.5$, the beam is self-focused which just compensates the spreading, as seen in Figs. 4(b) and 5(b). After some time, when the refractive index of the SWW core becomes larger than $n_{core} = 1.505$, the beam is completely self-trapped and creates a straight SWW, see Figs. 4(c) and 5(c).

3.3 Beam Splitting

We observed that when the saturation of the material mixture is reached, the SWWs break into filaments within the computation domain. A bent SWW is simulated using the diffusion based material model which is created from two counter propagating Gaussian beams with beam width of 50 µm and misalignment of 50 µm propagated through a distance of 5 mm. The simulation begins with a photopolymer mixture having 97% monomer and 3% photoinitiator. For this case, the maximum modulation in refractive index is calculated by $n_p - n_m$, i.e., it equals to 0.04. When the simulation runs further after the desired modulation in refractive index is achieved, the nearby region starts to get polymerized which results in breaking up of the intensity distributions into filaments, as shown in Fig. 6. The filaments are generated due to the absence of a cladding to the SWWs which results in no light guiding.

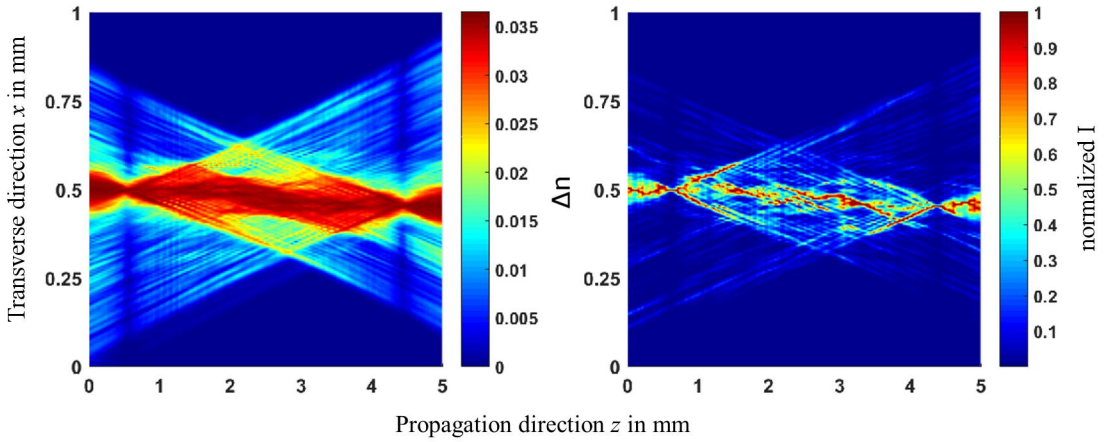

Figure 6. Filamentous nature of a bent SWW when the nearby region started to get polymerized. The result is obtained from the diffusion model.

4. SUMMARY AND CONCLUSION

In summary, a comparative study on theoretical predictions from two kinds of material models for simulating straight SWWs and bent SWWs is discussed. The results from the simple phenomenological model 1 nearly match with the results obtained from the more complex diffusion based material model 2, with few exceptions noticed in the uniformity and the bending of the SWWs. The SWWs created using the diffusion based material model show smoother, more uniform surfaces and more prominent bending compared to the SWWs created using the phenomenological model. The curing time of bent SWWs is provided for both models which showing that model 1 yields a faster increase in refractive index in comparison to model 2. Also, the self-written structures become filamentous when the nearby region starts to get polymerized as the evolution in refractive index is near to the maximum or saturation value of refractive index modulation.

ACKNOWLEDGMENTS

This research work was supported by the VolkswagenStiftung within the 'Niedersächsisches Vorab' program in the framework of the project Hybrid Numerical Optics (HYMNOS).

REFERENCES

[1] O. Kashin, E. Tolstik, V. Matusevich, and R. Kowarschik, "Numerical investigation of the (1+1)d self-trapping of laser beams in polymeric films based on polymethylmethacrylate and phenanthrenequinone," *J. Opt. Soc. Am. B* **26**, 2152–2156 (2009).

[2] R.Malallah, I.Muniraj, H.Li, D.Cassidy and J.Sheridan, "Interactions of two counter-propagating waveguides in the dry photopolymer material using fiber optics," *Frontiers in Optics* , JTh2A–146 (2016).

[3] H. Li, Y. Dong, P. Xu, Y. Qi, C. Guo, and J. Sheridan, "Beam self-cleanup by use of self-written waveguide generated by photopolymerization," *Opt. Lett.* **40**, 2981–2984 (2015).

[4] A. Günther, S. Schneider, M. Rezem, Y. Wang, U. Gleissner, T. Hanemann, L. Overmeyer, E. Reithmeier, M. Rahlves, and B. Roth, "Automated misalignment compensating interconnects based on self-written waveguides," *J. Lightwave Technol.* **35**, 2678–2684 (2017).

[5] A.Günther, A.Petermann, U.Gleissner, T.Hanemann, E.Reithmeier, M.Rahlves, M. Meinhardt-Wollweber, U.Morgner, and B. Roth, "Cladded self-written multimode step-index waveguides using a one-polymer approach," *Opt. Letter* **40**, 1830–1833 (2015).

[6] H.Li, Y.Qi, R.Malallah, J.P.Ryle, and J.T.Sheridan, "Self-trapping of optical beams in a self-written channel in a solid bulk photopolymer material," *Proc.SPIE* **9508**, 9508–7 (2015).

[7] A.A. Sukhorukov, S. Shoji, Y.S. Kivshar, "Self-written waveguides in photosensitive materials," *Journal of Nonlinear Optical Physics & Materials* **11**, 391–407 (2002).

[8] Ginés Lifante Pedrola, [*Beam Propagation Method for Design of Optical Waveguide Devices*], John Wiley & Sons (2015).

[9] H.Li, Y.Qi, R.Malallah, and J.Sheridan, "Modeling the Nonlinear Photoabsorptive Behavior during Self-Written Waveguide Formation in a Photopolymer," *J. Opt. Soc. Am. B* **32** (2015).

[10] Heller, W., "Remarks on refractive index mixture rules," *The J. Physical Chemistry* **69**, 1123–1129 (1965).

[11] T. Babeva, I. Naydenova, D. Mackey, S. Martin, and V. Toal, "Two-way diffusion model for short-exposure holographic grating formation in acrylamide-based photopolymer," *J. Opt. Soc. Am. B* **27**, 197–203 (2010).

[12] S.Gallego, A.Márquez, M.Ortuño, J.Francés, S. Marini, A.Beléndez, and I.Pascual, "Surface relief model for photopolymers without cover plating," *Opt. Express* **19**, 10896–10906 (2011).

[13] M. Ben Belgacem, S. Kamoun, M. Gargouri, K. Honorat Dorkenoo, A. Barsella, and L. Mager, "Light induced self-written waveguides interactions in photopolymer media," *Opt. Express* **23**, 20841–20848 (2015).

[14] T.M. Monro, L. Poladian, and C.M. De Sterke, "Analysis of self-written waveguides in photopolymers and photosensitive materials," *Phys. Rev. E* **57**, 1104–1113 (1998).